Catal Lett (2010) 135:83–90
DOI 10.1007/s10562-010-0272-9

Pt Catalyst Supported on Multi-Walled Carbon Nanotubes for Hydrogenation-Dearomatization of Toluene and Tetralin

**Hua Kong · Min Zhou · Guo-Dong Lin ·
Hong-Bin Zhang**

Received: 11 November 2009 / Accepted: 11 January 2010 / Published online: 2 February 2010

Abstract A type of MWCNT-supported Pt catalysts for the hydrogenation-dearomatization (HDA) of aromatics was developed, which displays excellent performance for HDA of two model compounds, toluene and tetralin. Over the 1%Pt/CNTs catalyst, near 100% conversion of toluene or tetralin was observed under the reaction temperature of 373 K. The specific reaction rate of HDA of toluene and tetralin reached 0.0524 and 0.0174 mmol s^{-1} $(m^2_{\text{-surf. Pt}})^{-1}$, respectively. Both of the values were 1.18 times those (0.0444 and 0.0148 mmol s^{-1} $(m^2_{\text{-surf. Pt}})^{-1}$, respectively) of the 2.4%Pt/AC catalyst with the optimal Pt loading under the same reaction conditions. It was experimentally found that using the CNTs in place of AC as the support of the catalyst did not cause a significant change in the apparent activation energy for the HDA reaction of toluene or tetralin, but led to a certain increase in the molar percentage of catalytically active Pt-species (Pt^0) in the total Pt-amount at the surface of the functioning catalyst. In addition, the Pt/CNTs catalyst could reversibly adsorb a greater amount of hydrogen under atmospheric pressure and temperatures ranging from room temperature to 773 K. This unique feature would help to generate a microenvironment with higher stationary state concentration of active hydrogen-adspecies at the surface of the functioning catalyst. These effects favored increasing the rate of the HDA reaction of toluene or tetralin.

Keywords MWCNTs · Platinum · Toluene · Tetralin · Hydrogenation-dearomatization

1 Introduction

Hydrogenation-dearomatization (HDA), together with hydro-desulfurization (HDS) and hydro-denitrification (HDN), is one of the important hydroprocessing processes of petroleum refining [1, 2]. The existing sulfided CoMo, NiMo and NiW catalysts for HDA reaction are active only at relatively high temperatures (e.g., >573 K). Thus complete hydrogenation of aromatics is not possible due to equilibrium limitations [3]. Noble metals are active for hydrogenation at lower temperatures, yet their use is limited because of their sensitivity to sulfur poisoning. In current processing schemes involving noble metal catalysts, two or more stages with multiple catalyst beds are used to achieve deep HDS and deep HDA. HDS occurs in the first stage over a CoMo or NiMo catalyst, followed by intermediate byproduct gas removal. Finally, HDA over the noble metal catalyst operates in the last stage, where the concentrations of catalyst poisons (organosulfur and H_2S) are extremely low [2, 4].

The commercial noble metal-based catalysts for deep hydrogenation of fuels are mostly supported on alumina. The ongoing efforts to search for new types of catalyst support and/or promoter so as to improve lower-temperature activity of the catalysts have been the focus of a lot of research and development activities [5].

Multi-walled carbon-nanotubes (symbolized as MWCNTs and simplified as "CNTs" in next text, unless otherwise specified) as a novel nano-carbon material have been drawing increasing attention in recent years [6–12]. This new form of carbon is structurally close to hollow

---

H. Kong · M. Zhou · G.-D. Lin · H.-B. Zhang (✉)
Department of Chemistry, College of Chemistry and Chemical Engineering, State Key Laboratory of Physical Chemistry for Solid Surfaces and National Engineering Laboratory for Green Chemical Productions of Alcohols-Ethers-Esters, Xiamen University, Xiamen 361005, China
e-mail: hbzhang@xmu.edu.cn

graphite fiber, except that it has a much higher degree of structural perfection. This type of carbon nanotubes possesses a series of unique features, such as graphitized tube-wall, nanometer-sized channel and sp^2-C-constructed surface. They display high thermal/electrical conductivity, medium to high specific surface areas, and excellent performance for adsorption of hydrogen, all of which render this kind of nanostructured carbon materials full of promise as a novel catalyst support and/or promoter.

Here we report the development of a type of CNT-supported Pt catalysts, which displays much better performance for highly effective HDA of the two model compounds, toluene and tetralin, in comparison with the reference Pt catalyst supported on activated carbon (AC).

2 Experimental

2.1 Catalyst Preparation

The CNTs were prepared from catalytic decomposition of CH_4 by the CCVD method reported previously [13]. The freshly prepared CNTs were purified by treatment of boiling nitric acid ($\sim$8 mol L^{-1}, at 373 K) for 16 h, followed by rinsing with de-ionized water twice, and then drying at 383 K in air. Open-end CNTs with somewhat hydrophilic surface were then obtained.

A series of Pt catalysts supported on the CNTs, denoted as x%(mass percentage)Pt/CNTs, were prepared by an incipient wetness method. An aqueous solution containing desired amount of platinum, which was prepared by dissolving the $H_2PtCl_6 \cdot 6H_2O$ (of AR grade, Shanghai Institute of Chem. Reagent) into calculated amount of HCl aqueous solution (0.2 mol L^{-1}), was impregnated onto the HNO_3-treated CNT-support, followed by laying up for 8 h, drying at 383 K for 6 h, and then cooling down to room temperature, thus yielding the CNT-supported Pt catalyst precursor in oxidation state.

The reference catalyst supported on AC, noted as x%Pt/AC, was prepared in a similar way. Prior to being used, the AC support (Xiamen Chem. Reagent Co., with 830 m^2 g^{-1} of N_2-BET-SSA) was pretreated first with 10% NaOH aqueous solution and then with 50% HNO_3 solution, followed by rinsing with de-ionized water and drying at 383 K. All samples of catalyst precursor were pressed, crushed, and sieved to a size of 40–80 mesh for the activity evaluation.

2.2 Catalyst Evaluation

Performance of the catalysts for the HDA of toluene or tetralin was evaluated in a fixed-bed continuous-flow reactor and gas chromatograph (GC) combination system. 50 mg of catalyst sample was used for each test. Prior to the reaction, the sample of the catalyst precursor was prereduced in situ under a $V(H_2){:}V(N_2) = 5{:}95$ stream at 0.16 MPa and 2,400 mL h^{-1} $g^{-1}_{\text{-catal.}}$. The reduction temperature was programmed to rise at a rate of 1 K min^{-1} from room temperature to 473 K and to maintain at that temperature for 3 h, and then to decrease to desired temperature for the catalyst test.

Hydrogenation-dearomatization reaction of the two model compounds was conducted at a stationary state under reaction conditions of 0.4 MPa, 373 K, feed: $H_2 = 6{:}94$ (mol ratio) and GHSV $= 120$ L h^{-1} $g^{-1}_{\text{-catal.}}$ for toluene, and of 0.16 MPa, 373 K, feed: $H_2 = 2{:}98$ (mol ratio) and GHSV $= 90$ L h^{-1} $g^{-1}_{\text{-catal.}}$ for tetralin, respectively. Feed was introduced into feed stream by flowing H_2 through a bubbler containing redistilled and purified liquid toluene or tetralin, and their concentration was regulated by controlling the temperature of the bubbler. Exit gas from the reactor was immediately brought down to atmospheric pressure and transported, while maintaining its temperature at 403 K, to the sampling valve of GC (Model GC-950 by Shanghai Haixin GC Instruments, Inc.), which was equipped with hydrogen flame ionization detector (FID) and a 1.0 m-long DNP column, and with N_2 as carrier gas, for online analysis. All data were taken after 4 h for toluene, or 11 h for tetralin, of stationary state operation. Conversions of toluene and tetralin were calculated by an internal normalization method.

2.3 Catalyst Characterization

Transmission electron microscope (TEM) and scanning electron microscope (SEM) observations, as well as energy dispersive spectra (EDS) observations were performed with JEM-2100 and LEO-1530 electron microscopes, respectively. X-ray photoelectron spectroscopy (XPS) measurements were done on a VG Multi-Lab 2000 machine with Mg Kα (300 W, $hv = 1253.6$ eV) under ultrahigh vacuum (10^{-7} Pa), calibrated internally by the carbon deposit C(1s) ($E_b = 284.6$ eV).

Test of H_2-temperature-programmed reduction (TPR) of catalyst precursor in oxidation state was conducted on a fixed-bed continuous-flow reactor-GC (Shimadzu GC-8A) combined system. 50 mg of the catalyst precursor in oxidation state was used for each test. The sample was first flushed by an Ar (of 99.999% purity) stream at 393 K for 60 min to clean its surface, and then cooled down to room temperature, followed by switching to a N_2-carried 5%H_2 gaseous mixture stream as reducing gas (30 mL min^{-1}) to start the TPR measurement from 298 to 773 K. The rate of temperature increase was 10 K min^{-1}. Change of hydrogen-signal was monitored using an on-line GC (Shimadzu GC-8A) with a thermal conductivity detector (TCD). A KOH (solid particles) $-$ column (φ5 mm $\times$ 100 mm-long) was installed at the reactor-exit to remove gaseous HCl and H_2O produced by H_2-reduction of the catalyst precursor.

The comparative investigations of adsorption of H_2 on the Pt catalysts supported on the different supports were conducted by using the H_2-temperature programmed desorption (TPD) method on a home-made adsorption–desorption/reaction system. 200 mg of catalyst sample was used for each test. Prior to TPD measurements, each sample was prereduced in situ in the TPD equipment by N_2-carried 5%H_2 gaseous mixture stream at the respective appropriate reduction temperature for the samples supported on the varying supports (i.e., 473 and 553 K for those supported the CNTs and AC, respectively) for 3 h, followed by cooling down to 373 K, switching to a H_2 (of 99.999% purity) stream for hydrogen adsorption at 373 K for 60 min and subsequently at room temperature for 240 min, and then flushing by the Ar stream at room temperature until the stable baseline of GC appeared. The rate of temperature increase was 10 K min^{-1}. Change of hydrogen-signal was monitored using an on-line GC (Shimadzu GC-8A) with a TC detector.

Specific surface area (SSA) was determined by N_2 adsorption using a Micromeritics Tristar-3000 (Carlo Erba) system. Measurement of CO chemisorption on the catalysts was performed by a Micromeritics ASAP-2010 Micropore Analyzer. From the determined amount of chemisorbed CO, the dispersion and surface area of metallic platinum were calculated [14]. 1.0 g of catalyst sample was used for each test. The sample was placed in a quartz tube, followed by evacuating for 10 min at 393 K, then switching to a N_2-carried 5%H_2 gaseous mixture stream (30 mL min^{-1}) as reducing gas to conduct an in situ H_2-TPR treatment of the catalyst sample, subsequently evacuating for 1 h at the reduction temperature and for 1 h more after cooling down to room temperature. It was then switched to gaseous CO (of 99.99% purity) to conduct the measurement of CO chemisorption following the specified procedure of the aforementioned analyzer. The results of the blank test showed that under the above-mentioned experimental conditions, the determined amounts of CO chemisorption on the two supports (the CNTs and AC) were all zero, indicating that the determined amounts of CO chemisorption on the corresponding supported Pt catalysts were contributed solely by CO chemisorption on the metal Pt surface.

3 Results and Discussion

3.1 Composition Optimization and Performance of Catalyst

With the HDA of toluene and tetralin as model reactions (Eqs. 1, 2), composition of the *x*%Pt/CNTs catalysts was optimized. The blank test showed that little HDA-activity of toluene or tetralin was detected over the sole support of CNTs in the temperature region of 353–423 K. Figure 1 shows the assay results of HDA reactivity of toluene and tetralin over the CNT-supported Pt catalysts with varying Pt-loading under the reaction temperature of 373 K. Conversion of toluene and tetralin both increased with increasing Pt-loading amount, and approached 100% at the Pt loading of 1.0% (mass percentage), indicating that the optimal Pt loading was 1.0%. Methylcyclohexane and decalin (with the molar ratio of *trans*-/*cis*-isomers being 27:73) was the only product of hydrogenation of toluene and tetralin, respectively, without other possible products detected.

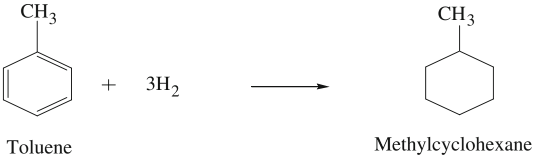

(1)

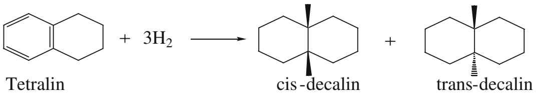

(2)

In order to investigate the effect of the CNT support on the performance of the catalyst, reactivity of HDA of toluene and tetralin over the Pt catalyst supported on the AC was evaluated and compared with that of the Pt catalyst supported on the CNTs. The results (Fig. 2) showed that the support could significantly affect the reactivity of HDA of toluene or tetralin. Under the respective reaction

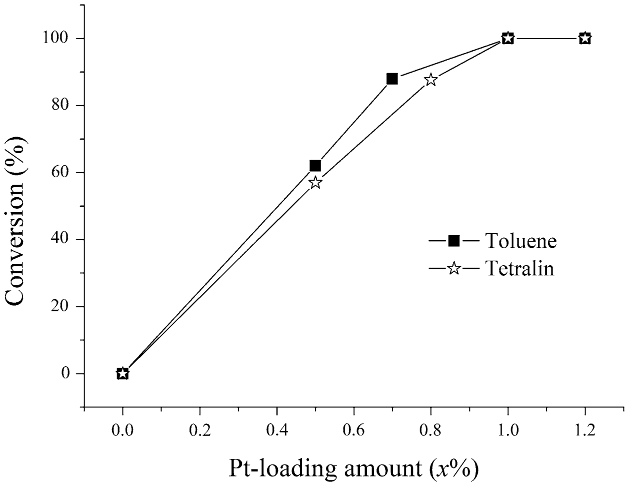

Fig. 1 Reactivity of HDA of toluene or tetralin over the *x*%Pt/CNTs catalyst with varying Pt-loading amount; reaction conditions: 0.4 MPa, 373 K, toluene: $H_2 = 6:94$ (molar ratio) and GHSV = 120 L h^{-1} $g^{-1}_{\text{-catal.}}$, or 0.16 MPa, 373 K, tetralin: $H_2 = 2:98$ (molar ratio) and GHSV = 90 L h^{-1} $g^{-1}_{\text{-catal.}}$

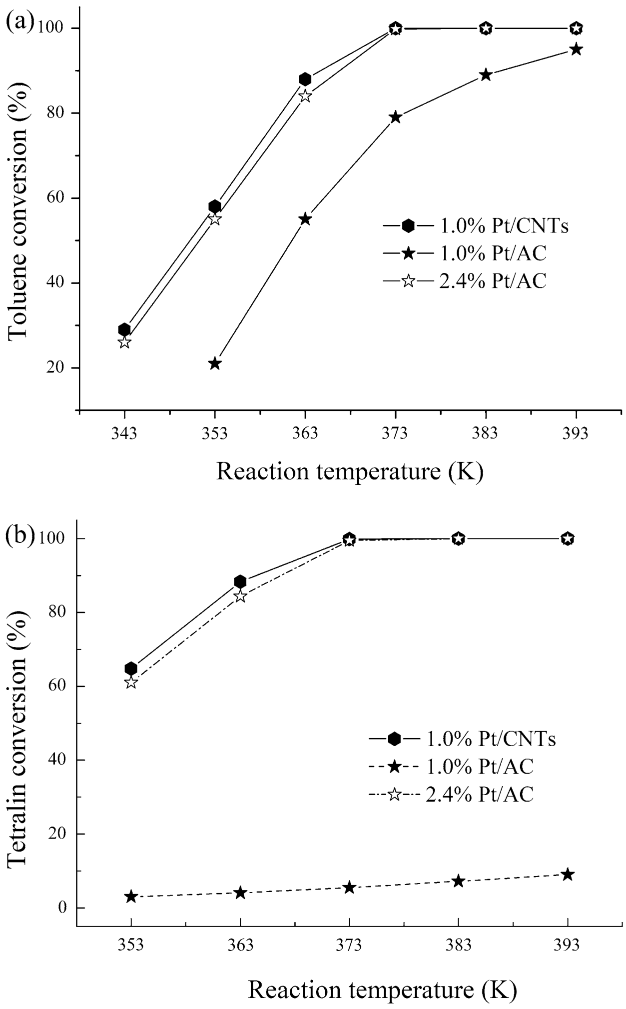

Fig. 2 Reactivity of HDA of toluene (**a**) or tetralin (**b**) over the Pt catalysts supported on CNTs and AC, respectively; reaction conditions are the same as in Fig. 1, except the reaction temperature

conditions of 353 K, conversion of toluene and tetralin reached 58.0% and 64.8%, respectively, over 1.0%Pt/CNTs, while merely 21.0% and 3.0%, respectively, over the counterpart supported on AC, 1.0%Pt/AC.

In view of the difference in the specific surface area between the two supports, the optimization of Pt-loading amount on the AC support was done. The results showed that the optimal Pt-loading amount was 2.4% for the AC. Over the 2.4%Pt/AC catalyst, the conversion of toluene and tetralin reached 55.0% and 61.0%, respectively (Fig. 2), under the aforementioned respective reaction conditions of 353 K. Note that in order to make both Pt catalysts achieve the same level of activity (i.e., near 100% of toluene or tetralin converted at 373 K), the Pt-loading amount needed on the AC was 2.4 times that of platinum needed on the CNTs.

In order to compare the catalytic efficiency produced by unit area of metal Pt surface of the catalysts supported on the varying supports, the specific reaction rate, i.e., the reaction rate of hydrogenation of toluene or tetralin on metallic Pt surface of unit area, was used as reference. It can be seen from Table 1 that under the aforementioned reaction conditions at 373 K, the specific reaction rate of HDA of toluene and tetralin reached 0.0524 and 0.0174 mmol s^{-1} $(m^2_{\text{-surf. Pt}})^{-1}$, respectively. Both of the values were 1.18 times those (0.0444 and 0.0148 mmol s^{-1} $(m^2_{\text{-surf. Pt}})^{-1}$, respectively) of the 2.4%Pt/AC catalyst under the same reaction conditions. This result suggested that the AC mainly played the role as support, while the CNTs played dual roles as support and promoter. The textural properties (specific surface area (SSA), Pt dispersion, metal Pt surface area) of the catalysts and the specific reaction rate of HDA of toluene and tetralin over the catalysts supported on the two kinds of supports are listed in Table 1.

The apparent activation energy (E_a) of HDA reaction of toluene and tetralin over these catalysts was measured under reaction conditions of 0.4 MPa, 353–393 K, toluene: H_2 = 6:94 (molar ratio), GHSV = 600 L h^{-1} $g^{-1}_{\text{-catal.}}$ and of 0.16 MPa, 353–393 K, tetralin: H_2 = 2:98 (mol ratio) and GHSV = 450 L h^{-1} $g^{-1}_{\text{-catal.}}$, respectively, with mass transfer limitation ruled out. The results were illustrated in Fig. 3. The E_a measured on the 1.0%Pt/CNTs catalyst was 41.4 and 37.4 kJ mol^{-1} for HDA of toluene and tetralin, respectively. These values were very close to 45.0 and 36.6 kJ mol^{-1} on the reference system supported on the AC, respectively. This indicated that using the CNTs in place of AC as support of the Pt catalyst displayed little change in the E_a for the HDA reaction of toluene or tetralin, most likely implying that the use of the CNTs in place of AC as support did not alter the main reaction pathway of HDA of toluene or tetralin.

Table 1 Specific reaction rate of HDA of toluene and tetralin over the Pt catalysts supported on CNTs and AC, respectively

Catalyst	SSA/m^2 $g^{-1}_{\text{-catal.}}$	Pt dispersion/%	Metallic Pt surf. area/m^2 $g^{-1}_{\text{-catal.}}$	Specific reaction rate[a]/mmol s^{-1} $(m^2_{\text{-surf. Pt}})^{-1}$	
				Toluene	Tetralin
1.0%Pt/CNTs	115	69.0	1.70	0.0524	0.0174
2.4%Pt/AC	744	34.0	2.01	0.0444	0.0148

[a] Defined as the reaction rate of hydrogenation of toluene or tetralin on metallic Pt surface of unit area; the reaction conditions were the same as in Fig. 1, except T = 373 K

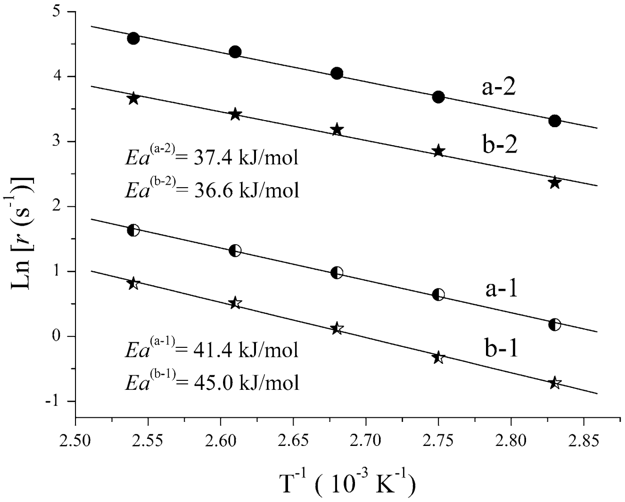

Fig. 3 Arrhenius plots of HDA of toluene (*1*) or tetralin (*2*) over the supported Pt catalysts: (*a*) 1.0%Pt/CNTs; (*b*) 2.4%Pt/AC; reaction conditions: 0.4 MPa, 353–393 K, toluene: H_2 = 6:94 (molar ratio), GHSV = 600 L h^{-1} $g^{-1}_{\text{-catal.}}$, or 0.16 MPa, 353–393 K, tetralin: H_2 = 2:98 (molar ratio) and GHSV = 450 L h^{-1} $g^{-1}_{\text{-catal.}}$

3.2 Characterization of Catalyst

3.2.1 Texture and Properties of CNTs

It is quite evident that the high reactivity of HDA of toluene and tetralin over the CNT-supported Pt catalyst is closely related to the unique structures and properties of the CNTs as support. The CNTs used in the present work were a “Herringbone type” of multi-walled carbon nanotubes [13, 15]. Previous characterization studies demonstrated that this type of CNTs were constructed by a superposition of many graphene layer facets, which were tilted at a certain angle with respect to the axis of the central hollow nanofibre, as if a number of cones were placed one on top of the other [13, 15]. Their outer diameters were in the range of 15–50 nm, the inner diameters in 3–7 nm and the N_2-BET surface area at about 130 m^2/g. The contents of element carbon and graphitized carbon were ≥99.5 and >90%, respectively, in the purified CNTs. Test of H_2-temperature-programmed hydrogenation (TPH) showed that the temperature needed for initiating the hydrogenation reaction of the CNTs with H_2 was ≥773 K [16], indicating that this type of CNTs was stable in H_2-atmosphere at the reaction temperatures for the HDA.

3.2.2 SEM/EDS and TEM Characterizations

Figure 4 showed SEM/TEM images and EDS of the 1.0%Pt/CNTs catalyst. It can be seen from Fig. 4a and b that the Pt nanoparticles dispersed well and scattered on the outer and inner surface of the CNTs. The Pt-particle diameters were estimated to be below 1 nm. The SEM/EDS analysis further demonstrated that carbon and oxygen were the two dominant elements at the surface of catalyst,

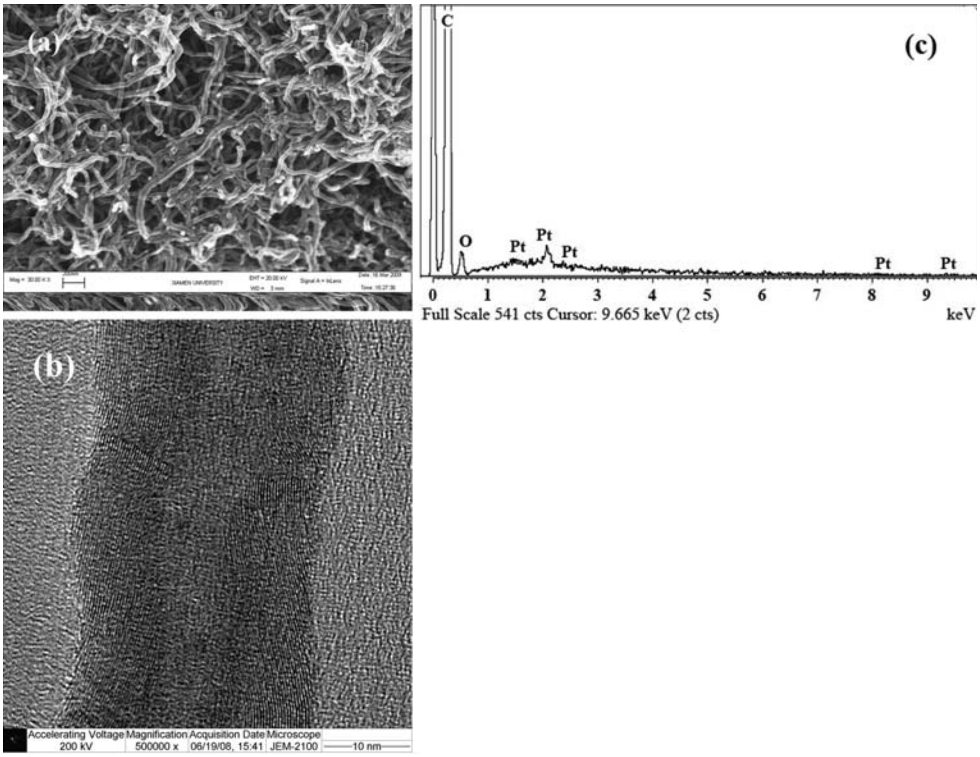

Fig. 4 SEM (**a**) and TEM (**b**) images and energy dispersive spectrum (EDS) (**c**) of 1.0%Pt/CNTs catalyst

with the content at 95.1% and 4.9% (atomic percentage), the corresponding mass percentage being 92.5% and 6.3%, respectively. The surface oxygen originated most probably from the pre-oxidation/carboxylation treatment of the CNTs by the concentrated nitric acid. The content of metal Pt made up of merely 0.08% (atomic percentage), with the corresponding mass percentage being 1.2%, in line with the formula for the preparation of the catalyst.

3.2.3 H_2-TPR Test

H_2-TPR study of the catalyst precursor in oxidation state provided useful information about its reducibility. Figure 5 shows the H_2-TPR profiles of the Pt catalyst precursors supported on the two supports. For 1.0%Pt/CNTs catalyst, the H_2-reduction initiated at 418 K, and rose to the peak at 498 K. This TPR peak may be ascribed to the continual multi-step single-electron reduction of Pt^{n+} species. For the AC-supported counterpart, the position of H_2-reduction peak went up to 506 K, but the total area-intensity of the TPR-profile (corresponding to a certain H_2-consumed amount) was estimated to be merely 78% of the value of the CNT-supported catalyst. The high specific H_2-consumed amount (i.e., the amount of hydrogen consumed due to reduction of unit mass of Pt) indicated the high percentage of the Pt^{n+} species reducible to lower valence in the total Pt amount. Based upon the difference in specific H_2-consumed amount and considering the temperature of the main H_2-reduction peak, it could be inferred that the order of reducibility of these supported Pt catalysts was as follows: 1.0%Pt/CNTs > 1.0%Pt/AC, in line with the order of the optimal reduction temperature for the two systems, i.e., 473 and 553 K for 1.0%Pt/CNTs and 1.0%Pt/AC, respectively.

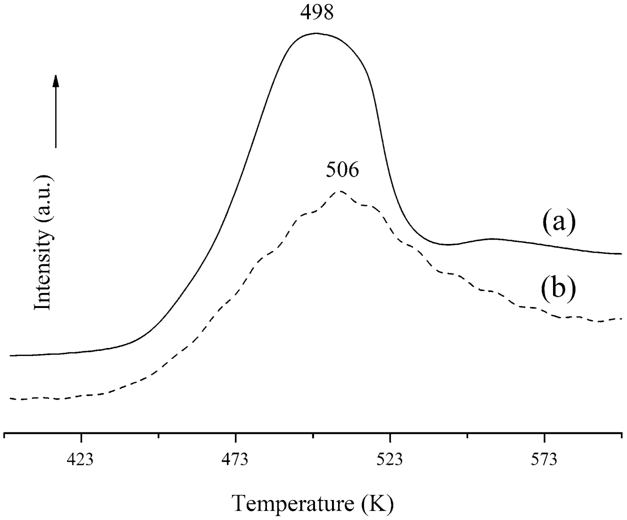

Fig. 5 H_2-TPR profiles of catalysts: (*a*) 1.0%Pt/CNTs; (*b*) 1.0%Pt/AC

3.2.4 XPS-Analysis

X-ray photoelectron spectroscopy-analysis of the tested catalysts revealed that certain differences existed between the two catalysts supported on the different carbon-supports in the valence-states of the surface Pt species and their molar percentage. Figure 6 showed the Pt(4*f*)-XPS spectra of the tested catalysts. With reference to Ref. [17–19] and through computer-fitting, it could be found that each of those Pt(4*f*)-XPS spectra involved the contribution from three kinds of surface Pt-species: Pt^0, Pt^{2+} and Pt^{4+} (see Fig. 6; Table 2). At the surface of the tested 1%Pt/CNTs catalyst, the molar percentage of Pt^0-species in the total Pt-amount reached 97.3 atomic%, being 1.12 times that (86.8 atomic%) of the AC-supported catalysts,

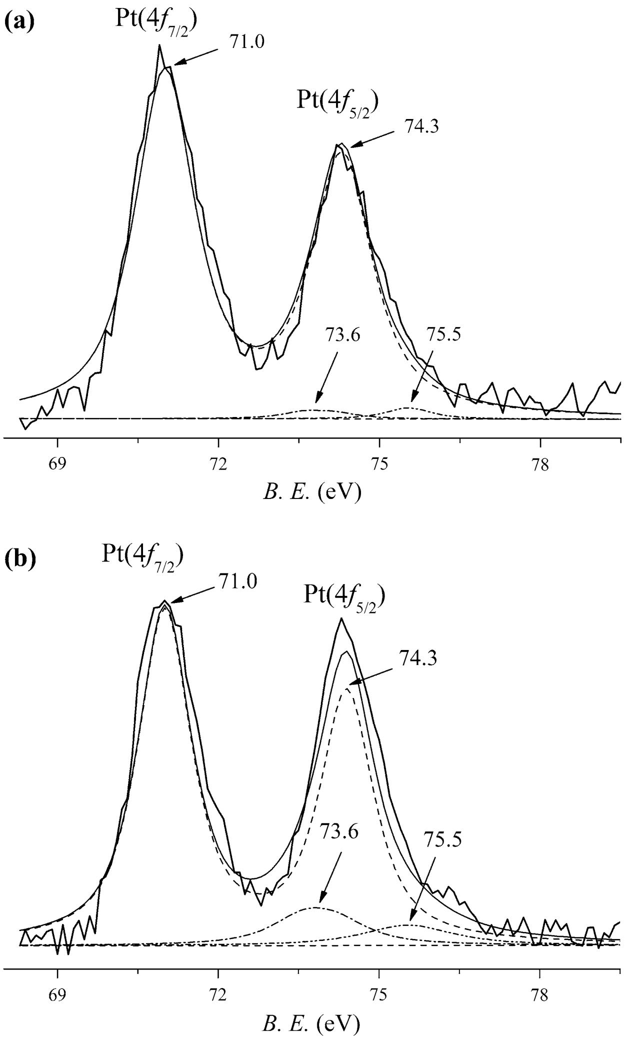

Fig. 6 Pt(4*f*)-XPS spectra of the tested catalysts: (**a**) 1.0%Pt/CNTs; (**b**) 2.4%Pt/AC

Table 2 XPS binding energy and molar percentage of the Pt-species with different valence states in the total Pt-amount at the surface of tested catalysts

Catalyst	E_b of Pt($4f_{7/2}$) (eV)			Relative content (atomic %)		
	Pt^0	Pt^{2+}	Pt^{4+}	Pt^0	Pt^{2+}	Pt^{4+}
1.0%Pt/CNTs	71.0	73.6	75.5	97.3	1.3	1.3
2.4%Pt/AC	71.0	73.6	75.5	86.8	8.1	5.1

2.4%Pt/AC. It followed that the sequence of relative concentration of the Pt^0-species at the surface of the two catalysts was: 1%Pt/CNTs > 2.4%Pt/AC. This result suggests that using the CNTs in place of the AC as support of the catalyst leads to a certain increase in the molar percentage of catalytically active Pt-species (Pt^0) in the total Pt-amount at the surface of the functioning catalyst.

This result of XPS-analysis was consistent with the aforementioned result of H_2-TPR measurement. It was one of the important reasons that led to the significant difference between the two types of catalysts, 1%Pt/CNTs and 2.4%Pt/AC, in their specific catalytic activity for HDA reaction of toluene or tetralin (i.e., reaction rate of hydrogenation of toluene or tetralin on the Pt of unit mass). It also provides new evidence to the generally accepted viewpoint that Pt^0 is the catalytically active Pt species for HDA of aromatics.

3.2.5 H_2-TPD Test

The results of H_2-TPD investigation showed that significant difference existed among the Pt catalysts supported on the CNTs and AC, respectively, in their adsorption/desorption behavior toward hydrogen. Figure 7 showed the H_2-TPD profiles of H_2 adsorption on these supported Pt catalysts in pre-reduced state. On the AC-supported Pt catalysts, desorption of H-adspecies started at 523 K, approached a peak at 673 K, and ended at 823 K. On the CNT-supported Pt catalyst, a shoulder-peak spanned from 338 to 593 K, resulting from the desorption of weakly adsorbed H-species, probably including molecularly adsorbed hydrogen and weakly dissociatively adsorbed hydrogen. In addition, a main peak at 768 K due to desorption of strongly adsorbed H-species, most probably dissociatively chemisorbed hydrogen, was observed.

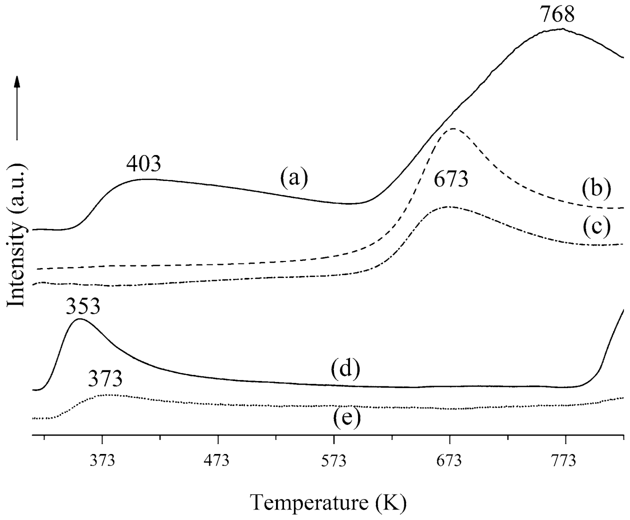

Fig. 7 H_2-TPD profiles of catalysts: (*a*) 1.0%Pt/CNTs; (*b*) 2.4%Pt/AC; (*c*) 1.0%Pt/AC; (*d*) CNTs; (*e*) AC

Considering that the hydrogenation of some surface carbon by H-adspecies (which would lead to consumption of part of H-adspecies and formation of C_{1-2}-hydrocarbons) could occur at temperatures of 773 K and above [20], we used the temperature range of 323–773 K for estimation and comparison of the area-intensity (corresponding to a certain amount of desorbed hydrogen) of these H_2-TPD profiles. The result showed that the ratio of relative area-intensity of these H_2-TPD profiles was: $S_{1.0\%Pt/CNTs}/S_{2.4\%Pt/AC}/S_{1.0\%Pt/AC} =$ 100/48/36. This was also expected to be the sequence of increase in concentration of hydrogen ad-species at the surface of functioning catalysts, in line with the activity sequence observed on the corresponding catalysts for the HDA of toluene and tetralin.

3.3 Nature of Promoter Action by CNTs

The aforementioned results of the evaluation and characterization of catalysts showed that using the CNTs in place of AC as support of the Pt catalyst could significantly enhance the catalyst activity for HDA of toluene or tetralin, yet it did not cause a marked change in the apparent activation energy (E_a) for the HDA reaction of toluene or tetralin. On the other hand, the H_2-TPR and XPS results showed that the CNT-supported Pt catalyst was more easily reduced by H_2 at relatively low temperature, and that the molar percentage of catalytically active Pt species (Pt^0) in the total Pt-amount at the surface of the functioning catalyst was relatively high, compared to that of the Pt catalyst supported on AC. This was undoubtedly in favor of enhancing the specific activity of the catalyst. Nevertheless, it would be difficult to justify, solely based on the difference in the metallic Pt exposed area (Pt^0-SA), the 18% increase in the specific reaction rate of HDA of toluene or tetralin for 1.0%Pt/CNTs vs. 2.4%Pt/AC (see Table 1).

In recent years there have been considerable experimental and theoretical investigations in the use of nanostructured carbon materials as potential hydrogen sorbents. It was demonstrated by Ishikawa et al. [21] that graphitized carbon black surfaces were capable of rapidly equilibrating H_2/D_2 mixture. A dissociation rate of

2.5×10^{17} molecules s^{-1} (m^2-ASA)$^{-1}$ (ASA—active surface area) was measured at ambient temperatures and pressures, regardless of the nature of the carbon material under investigation. The ASA was described in terms of atoms located at edge positions on the graphite basal plane and was determined from the amount of oxygen able to chemisorb at these sites. The H_2-TPD investigation by Zhou et al. [20] revealed that hydrogen adsorption on the CNTs can occur at ambient temperature and pressure, with adsorption of most (99%) of H_2 being reversible. It was also found that the desorbed product was almost exclusively gaseous hydrogen at temperatures lower than 723 K and involved CH_4, C_2H_4 and C_2H_2, in addition to H_2, at temperatures of 773 K and above, implying that H_2 adsorption on the CNTs may be in the two forms: associative (molecular state) and dissociative (atomic state). This has also been evidenced by the following-up LRS characterization of H_2/CNTs adsorption system [22].

It is clear that the high reactivity, especially the high specific reaction rate, of HDA of toluene and tetralin over the CNT-supported catalyst is closely related to the peculiar properties of the CNTs as support, especially their excellent performance for adsorption/activation of H_2 (see Fig. 7d). Based on the above H_2-TPD results, we suggest that there exists a considerably larger amount of reversibly adsorbed H-species on the CNT-supported Pt catalyst under the reaction conditions for the HDA of toluene and tetralin. This would generate a surface micro-environment with high stationary-state concentration of H-adspecies at the surface of the functioning catalyst, especially at the Pt_x^0 active-sites, since the highly conductive CNTs may promote hydrogen spill-over from the CNTs to the Pt_x^0 active-sites, and thus be favorable to increasing the rate of the HDA reaction of toluene and tetralin. This is very similar to the cases in synthesis of methanol from CO hydrogenation over the CNT-promoted Cu–ZnO–Al_2O_3 [23, 24] or from CO_2 hydrogenation over CNT-promoted Pd–ZnO [25]. In contrast, due to the lacking of the graphene-like structure and surface consisted of *sp*^{2}-C, AC may simply act as the catalyst support with low capability of adsorbing H_2 (see Fig. 7e) and thus rather limited promoter effect.

4 Concluding Remarks

In the developed CNT-supported Pt catalysts for HDA of toluene and tetralin, the CNTs played dual roles as a catalyst support and a promoter. The CNT-supported/promoted Pt-catalyst displays excellent performance for highly effective HDA of toluene or tetralin. Using the CNTs in place of AC as the catalyst support resulted in an increase of the molar percentage, in the total Pt-amount at surface of the functioning catalyst, of the catalytically active Pt^0-species closely associated with HDA of toluene and tetralin. On the other hand, it also markedly improves the capability of catalyst for adsorbing and activating H_2 (one of the reactants). Both these factors are favorable to increasing the rate of HDA reaction of toluene or tetralin.

Acknowledgments The authors are grateful for the financial supports from National Basic Research (“973”) Project (No. 2009CB939804) of China.

References

1. Cooper BH, Donnis BBL (1996) Appl Catal A Gen 137(2):203–223
2. Song CS, Ma XL (2003) Appl Catal B Environ 41(1–2):207–238
3. Stanislaus A, Cooper BH (1994) Catal Rev Sci Eng 36(1):75–123
4. Stork WHJ (1996) Deactivation and testing of hydrocarbon processing catalysts. ACS symposium series 634, pp 380–400
5. Lee JJ, Han S, Kim H, Koh JH, Hyeon T, Moon SH (2003) Catal Today 86:141–149
6. de Jong KP, Geus JW (2000) Catal Rev Sci Eng 42(4):481–510
7. Serp P, Corrias M, Kalck P (2003) Appl Catal A Gen 253(2):337–358
8. Zhang HB, Lin GD, Yuan YZ (2005) Curr Topics Catal 4:1–21
9. Zhang HB, Liang XL, Dong X, Li HY, Lin GD (2009) Catal Surv Asia 13(1):41–58
10. Li C-H, Yu Z-X, Yao K-F, Ji S, Liang J (2005) J Mol Catal A Chem 226(1):101–105
11. Wang Y, Shah N, Huggins FE, Huffman GP (2006) Energy Fuels 20:2612–2615
12. Hull RV, Li L, Xing YC, Chusuei CC (2006) Chem Mater 18:1780–1788
13. Chen P, Zhang HB, Lin GD, Hong Q, Tsai KR (1997) Carbon 35(10–11):1495–1501
14. Webb PA, Orr C (1997) Analytical methods in fine particle technology. Micromeritics Instrument Corporation, Norcross, p 260
15. Chen P, Zhang HB, Lin GD, Tsai KR (1998) Chem J Chin Univ 19(5):765–769
16. Zhou JM, Wang Y, Tang PP, Wu XM, Lin GD, Zhang HB (2005) Chin J Appl Chem 22(2):117–122
17. Liu ZL, Guo B, Hong L, Jiang HX (2005) J Photochem Photobiol A 172(1):81–88
18. Yao YL, Zhang D, Xia XH (2004) Chin J Inorg Chem 5(20):531–535
19. Matsumoto T, Komatsu T, Nakano H, Arai K, Nagashima Y, Yoo E, Yamazaki T, Kijima M, Shimizu H, Takasawa Y, Nakamura J (2004) Catal Today 90(3–4):277–281
20. Zhou ZH, Wu XM, Wang Y, Lin GD, Zhang HB (2002) Acta Phys Chem Sin 18(8):692–698
21. Ishikawa Y, Austin LG, Brown DE, Walker Jr PL (1975) In: Walker Jr PL, Thrower PA (eds) Chemistry and physics of carbon, vol 12. Marcel Dekker, New York, p 39
22. Zhang HB, Lin GD, Zhou ZH, Dong X, Chen T (2002) Carbon 40(13):2429–2436
23. Zhang HB, Dong X, Lin GD, Yuan YZ, Zhang P, Tsai KR (2003) Utilization of greenhouse gases. ACS symposium series 852, pp 195-209
24. Dong X, Zhang HB, Lin GD, Yuan YZ, Tsai KR (2003) Catal Lett 85(3–4):237–246
25. Liang XL, Dong X, Lin GD, Zhang HB (2009) Appl Catal B Environ 88(3–4):315–322